$t\bar{t}$ in BSM Phase space

Sandra Consuegra Rodríguez (RWTH Aachen) on behalf of the CMS Collaboration

17th International Workshop on Top Quark Physics (TOP2024), Saint-Malo, 22-27th September 2024

Motivation

- **Precision measurements of top quark pair ($t\bar{t}$) production**
  - ⋆ stringent tests for validity of SM
  - ⋆ crucial role in search for new phenomena
- **Large $t\bar{t}$ data sample collected at the CERN LHC**
  - ⋆ several measurements of differential cross sections for various $t\bar{t}$ decay channels & different center-of-mass energies
- **All measurements performed as function of kinematic observables of:**
  - ⋆ visible part of event (e.g. jets or charged leptons)
  - ⋆ intermediate particles [e.g. (anti-)top quark or W boson]

Motivation

- **For some BSM scenarios invisible part of event modified**
  - ⋆ precise & direct measurements of undetected particles in event (e.g. neutrinos)

↓

Crucial role in search for new phenomena

$t\bar{t}$ production in dileptonic final state

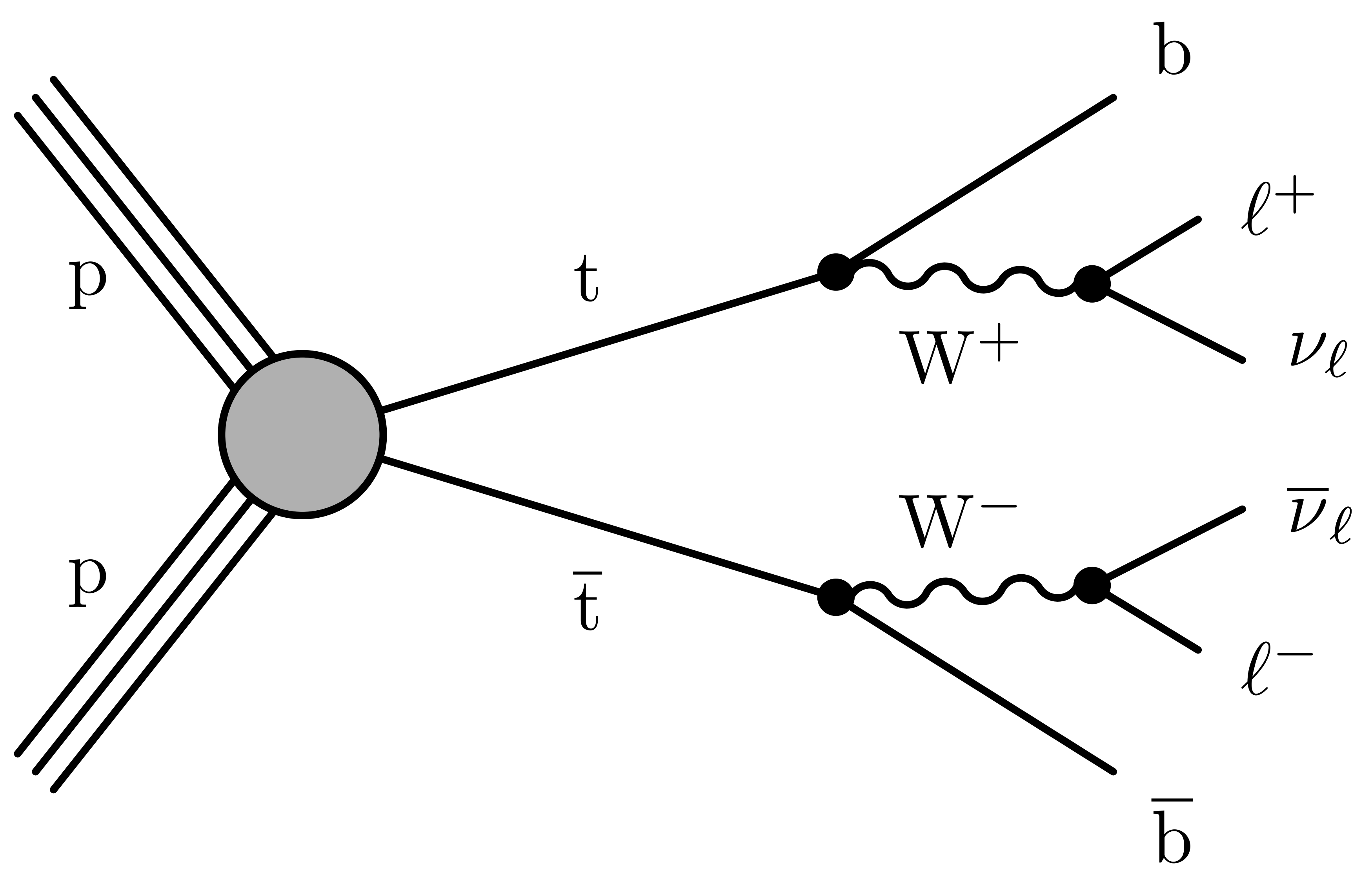

Top s-quark production

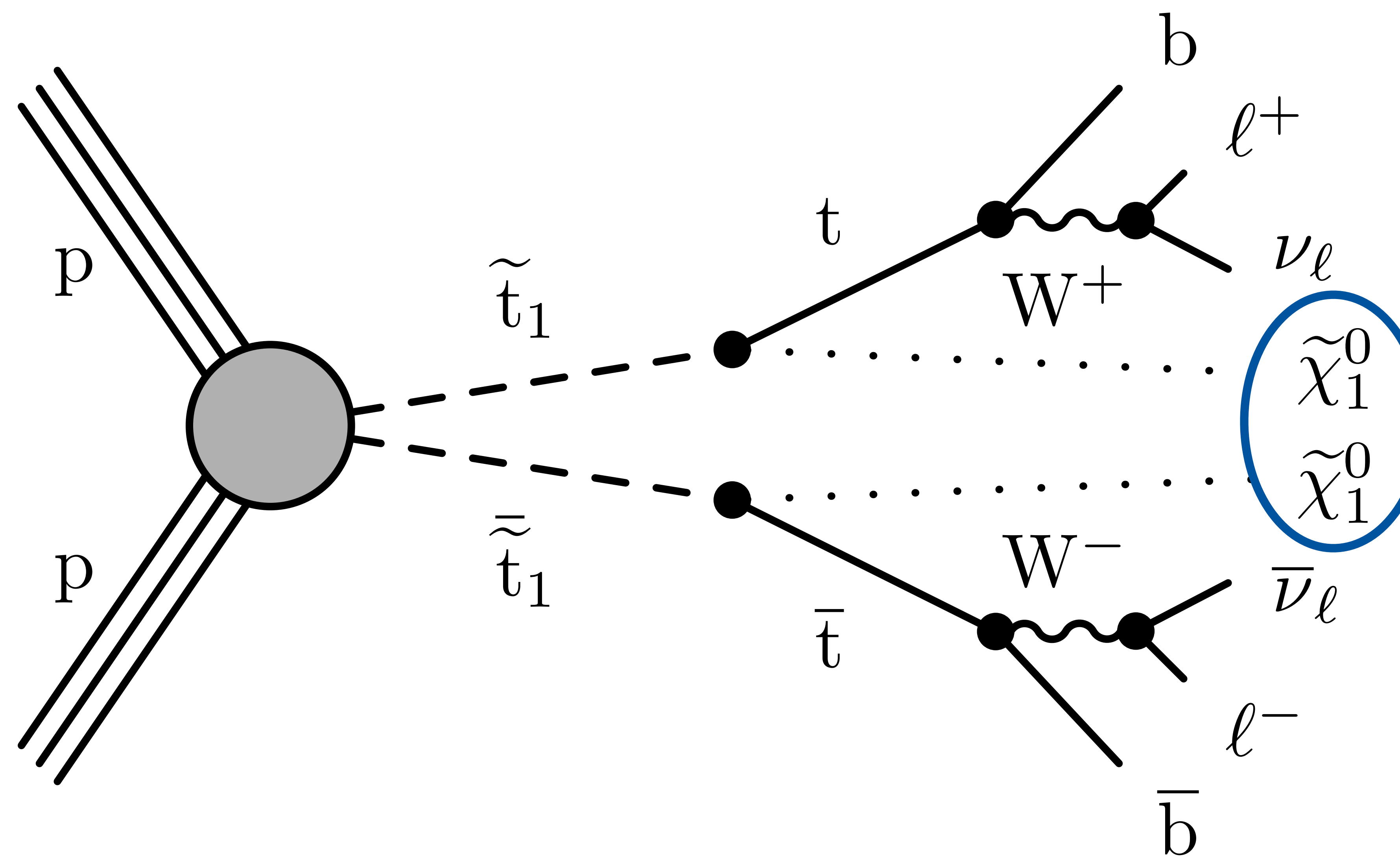

→ presence of $\tilde{\chi}_1^0$ modifies kinematics of invisible part of BSM event

Introduction

PAS-TOP-24-001

Physics briefing

- **First measurement of differential $t\bar{t}$ cross section as a function of:**
  - ⋆ transverse momentum of dineutrino system $p_{\mathrm{T}}^{\nu\nu}$
  - ⋆ minimum azimuthal distance between $\vec{p}_{\mathrm{T}}^{\nu\nu}$ and leptons: $\min[\Delta\phi(\vec{p}_{\mathrm{T}}^{\nu\nu}, \vec{p}_{\mathrm{T}}^{\ell})]$
  - ⋆ two-dimensional measurement of both observables
- **Selection of observables**
  - ⋆ driven by distinction between SM $t\bar{t}$ process & potential BSM scenarios with comparable signature but including additional sources of undetected particles
- **Main differences wrt “nominal” differential measurements:**
  - ⋆ Focus on observables related to dineutrino system $\vec{p}_{\mathrm{T}}^{\mathrm{miss}}$
  - ⋆ Dedicated DNN regression to improve $\vec{p}_{\mathrm{T}}^{\mathrm{miss}}$ resolution for dileptonic $t\bar{t}$ events

Event selection

- **at least two reconstructed jets**, $p_T > 30$ GeV, |η| < 2.4, **at least one b-tagged**
- **two charged leptons (electrons, muons)** of opposite charge (**dilepton channel**)
- $|\eta| < 2.4$, $p_T > 25$ (20) GeV for (sub)leading lepton
- veto on events with additional leptons (electrons or muons) with $p_T > 15$ GeV
- Events further separated into two **channels:**
    - $e^+e^-/\mu^+\mu^-$ **same-flavor (SF)**
    - $e^\pm\mu^\mp$ **different-flavor (DF)**

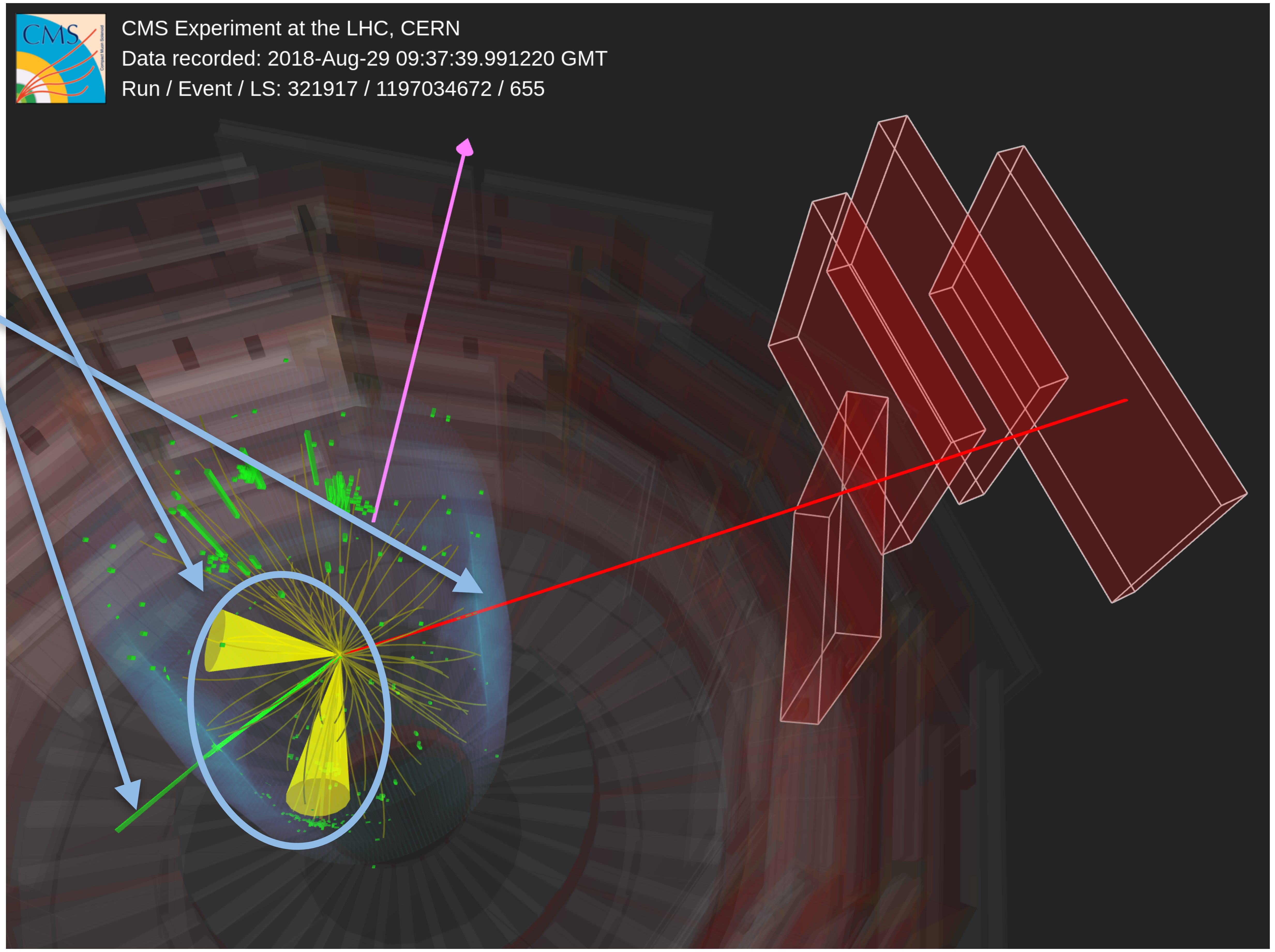

CMS-PHO-EVENTS-2024-027-3

[PAS-TOP-24-001]

Distributions after event selection

- Clean selection with overall ~78% signal contribution
- Largest background contributions from $t\bar{t}$ other, single top, and DY+jets

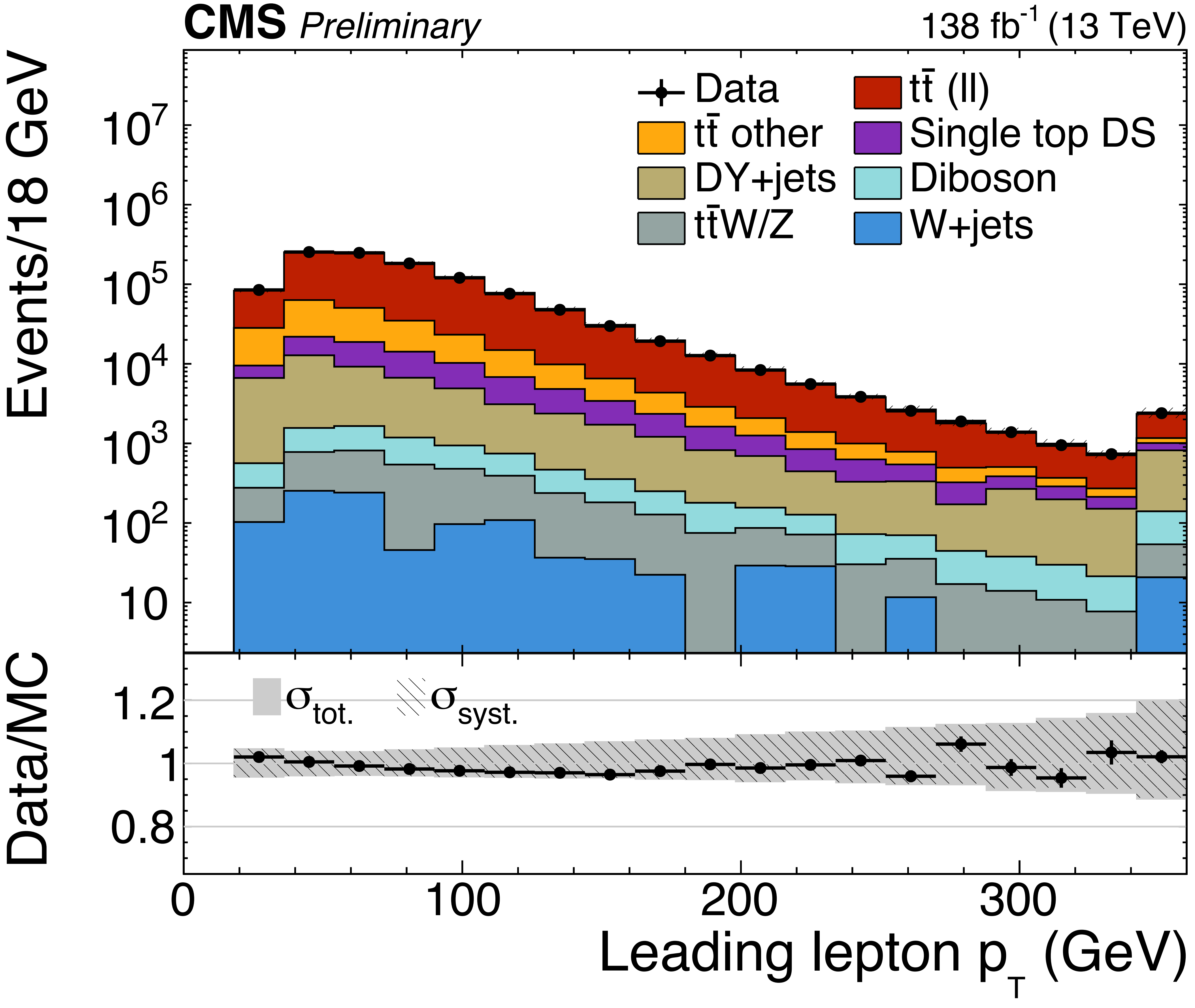

Figure_002-a

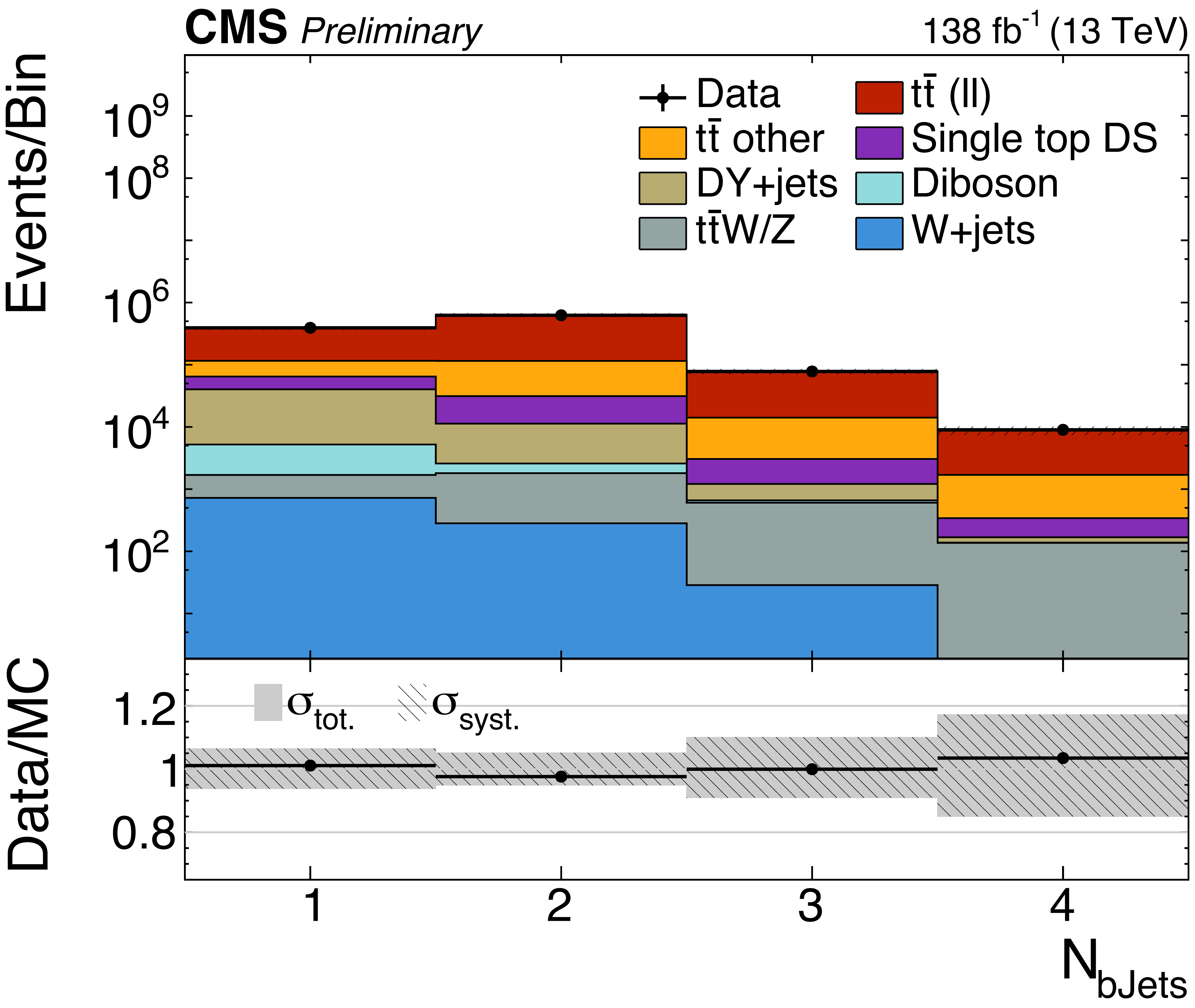

Figure_002-d

- Excellent Data/MC agreement, for individual channels & combination, and across different distributions

$\vec{p}_{T}^{\,miss}$ resolution

- **Sources of $\vec{p}_{T}^{\,miss}$:**
  - ⋆ the two prompt neutrinos produced in dileptonic $t\bar{t}$ decays ($p_{T}^{\nu\nu}$)
  - ⋆ non-prompt neutrinos from semileptonic meson decays in jets
  - ⋆ mismeasurement of particle momenta during reconstruction

    (largest impact arising from mismeasurements in jets)

- **Poor resolution or large biases of reconstructed $\vec{p}_{T}^{\,miss}$**
  - ⋆ stability of unfolding procedure can be compromised

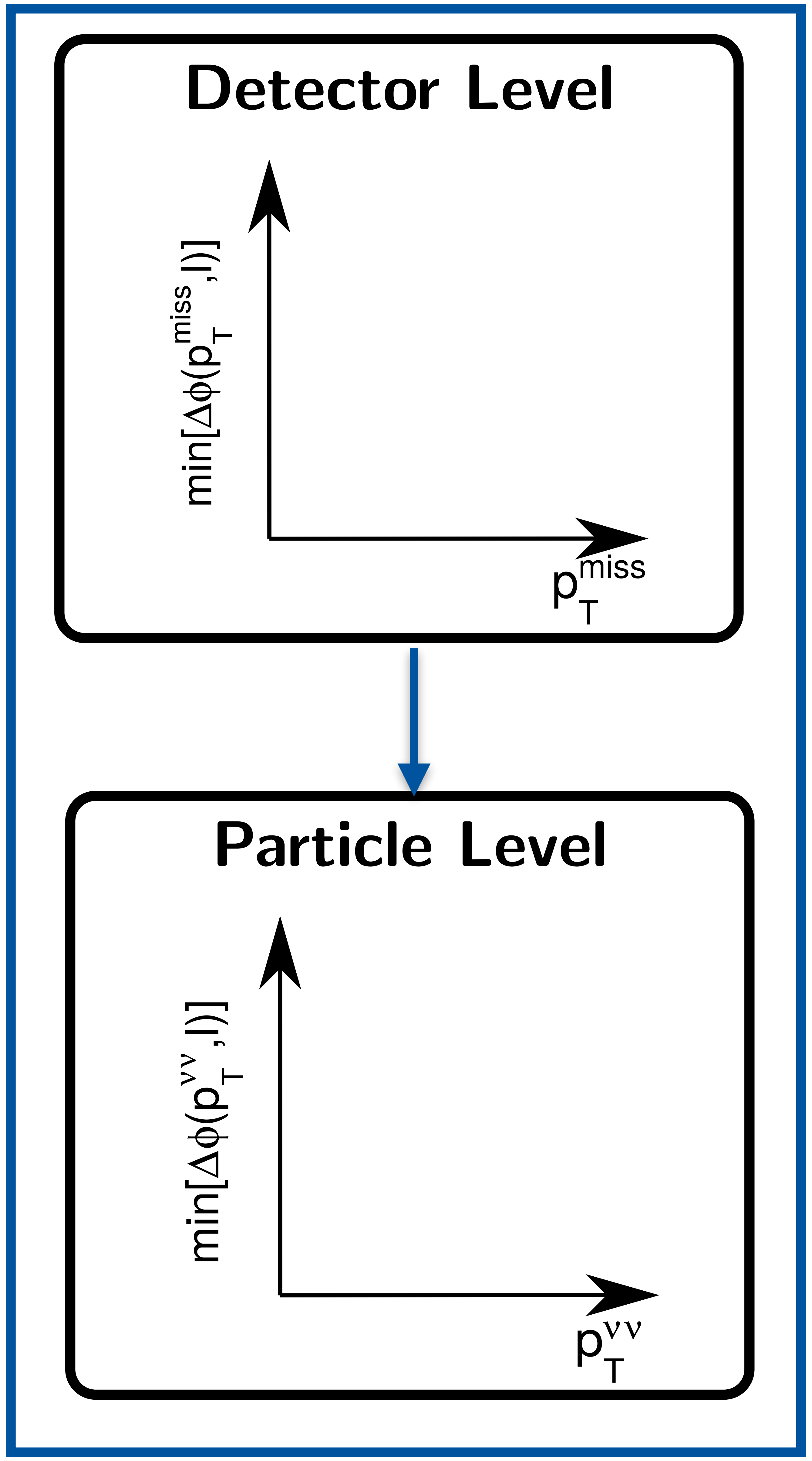

PAS-TOP-24-001

Improving $\vec{p}_{\mathrm{T}}^{\mathrm{miss}}$ resolution

- **DNN regression to correct $\vec{p}_{\mathrm{T}}^{\mathrm{miss}}$ for detector effects**
  - ⋆ ensure accurate reconstruction of its magnitude & direction
- **Feed-forward, fully-connected DNN with two output nodes:**
  - ⋆ x & y components of difference between:

$$\vec{p}_{\mathrm{T,PUPPI}}^{\mathrm{miss}} \;\&\; \vec{p}_{\mathrm{T,gen.}}^{\mathrm{miss}}$$

(simultaneously correct direction & magnitude of $\vec{p}_{\mathrm{T}}^{\mathrm{miss}}$)

- Resolution of $\vec{p}_{\mathrm{T}}^{\mathrm{miss}}$ improved by ~15% wrt $\vec{p}_{\mathrm{T,PUPPI}}^{\mathrm{miss}}$
- Resolution of $\phi(\vec{p}_{\mathrm{T}}^{\mathrm{miss}})$ improved by ~12%
  - ⋆ finer binning in differential measurements of target observables thanks to bin-to-bin migration reduction while keeping an stable unfolding

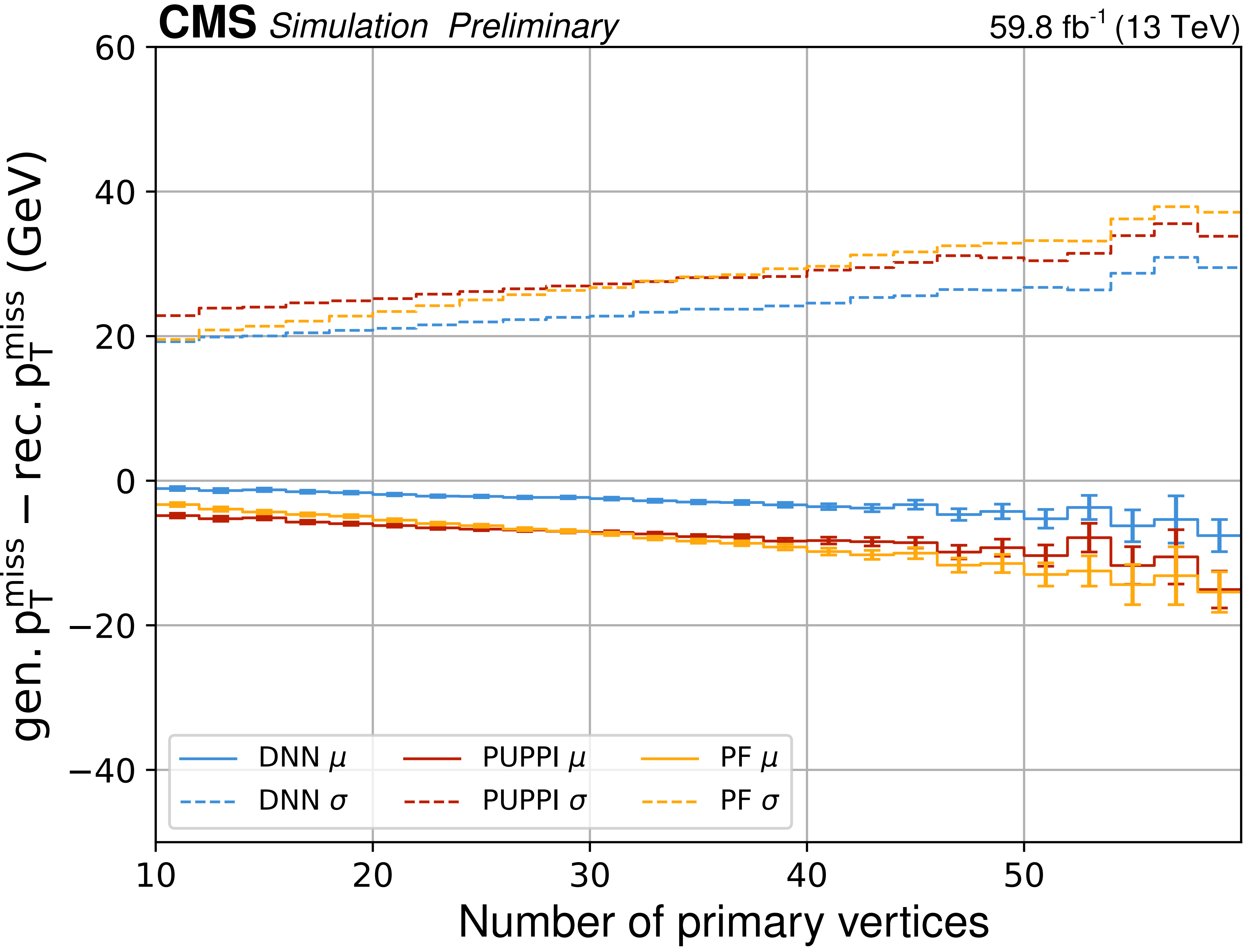

Figure_003-b

- **DNN:** $\vec{p}_{\mathrm{T}}^{\mathrm{miss}}$ corrected by DNN regression
- Puppi: $\vec{p}_{\mathrm{T}}^{\mathrm{miss}}$ pileup-per-particle identification
- PF: $\vec{p}_{\mathrm{T}}^{\mathrm{miss}}$ from particle flow algorithm

PAS-TOP-24-001

Experimental uncertainties

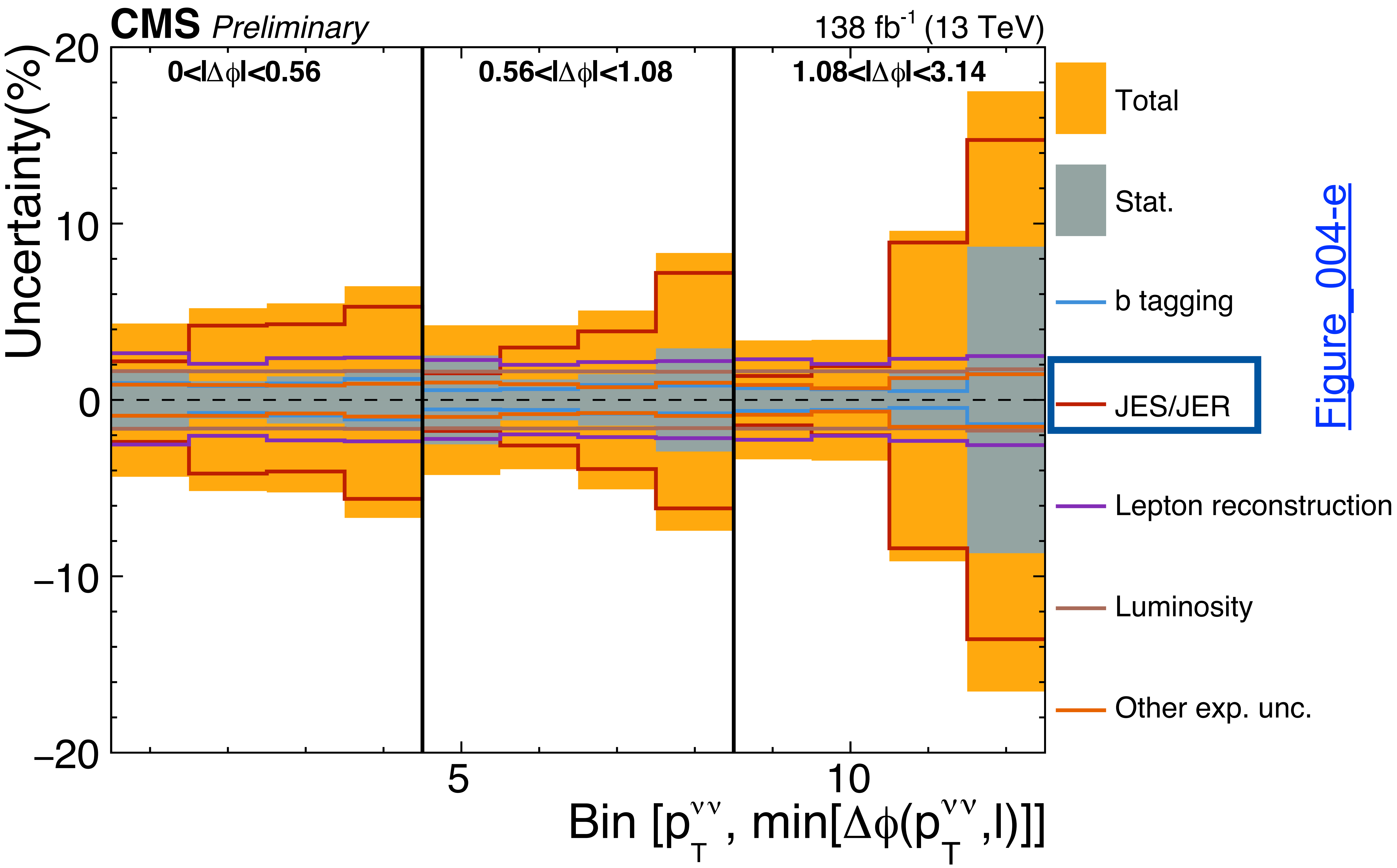

Figure_004-e

- $p_{\mathbf{T}}^{\nu\nu}$ **& 2D distribution**
  - ⋆ Jet Energy Scale (JES) dominant uncertainty for most bins
- **min**$[\Delta\phi(\vec{p}_{\mathbf{T}}^{\,\nu\nu}, \vec{p}_{\mathbf{T}}^{\,\ell})]$
  - ⋆ JES uncertainty dominant at low values
  - ⋆ Lepton reconstruction efficiency

[PAS-TOP-24-001]

Theory uncertainties

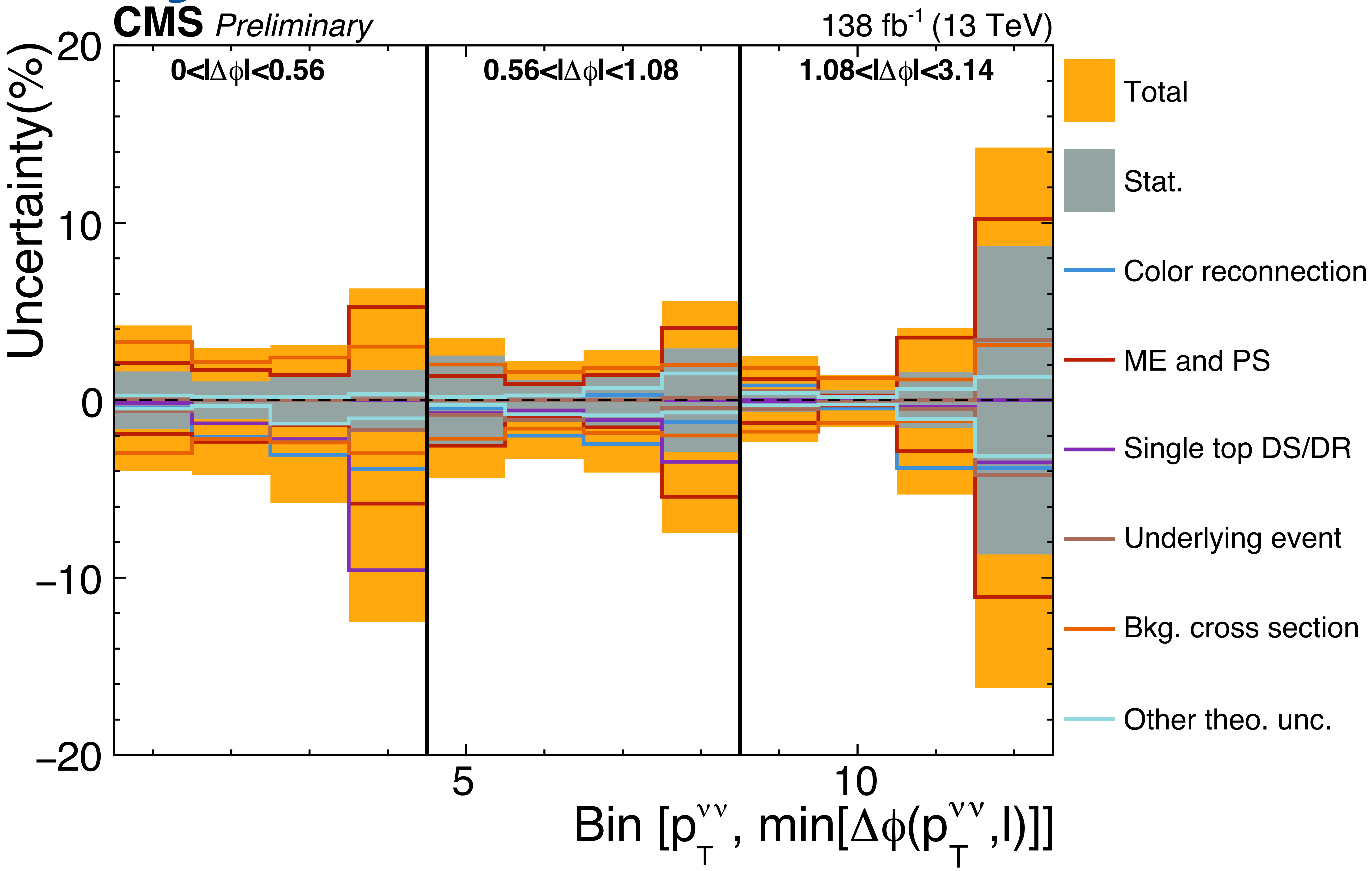

[Figure_004-f]

- $p_{\mathbf{T}}^{\nu\nu}$
  - ⋆ At large values:
    - choice of tW–$t\bar{t}$ overlap removal scheme
    - normalization of single top production background
    - Matrix element (ME) scale
- **min**$[\Delta\phi(\vec{p}_{\mathbf{T}}^{\nu\nu}, \vec{p}_{\mathbf{T}}^{\ell})]$
  - ⋆ At large values:
    - choice of tW–$t\bar{t}$ overlap removal scheme

- **2D distribution**
  - ⋆ Large $p_{\mathrm{T}}^{\nu\nu}$, lowest min$[\Delta\phi(\vec{p}_{\mathrm{T}}^{\nu\nu}, \vec{p}_{\mathrm{T}}^{\ell})]$ bin: choice of tW–$t\bar{t}$ overlap removal scheme
  - ⋆ Highest $p_{\mathrm{T}}^{\nu\nu}$ bin & min$[\Delta\phi(\vec{p}_{\mathrm{T}}^{\nu\nu}, \vec{p}_{\mathrm{T}}^{\ell})]$ bin: sizeable contributions from ME-Parton Shower matching and ME scale

Detector level distributions

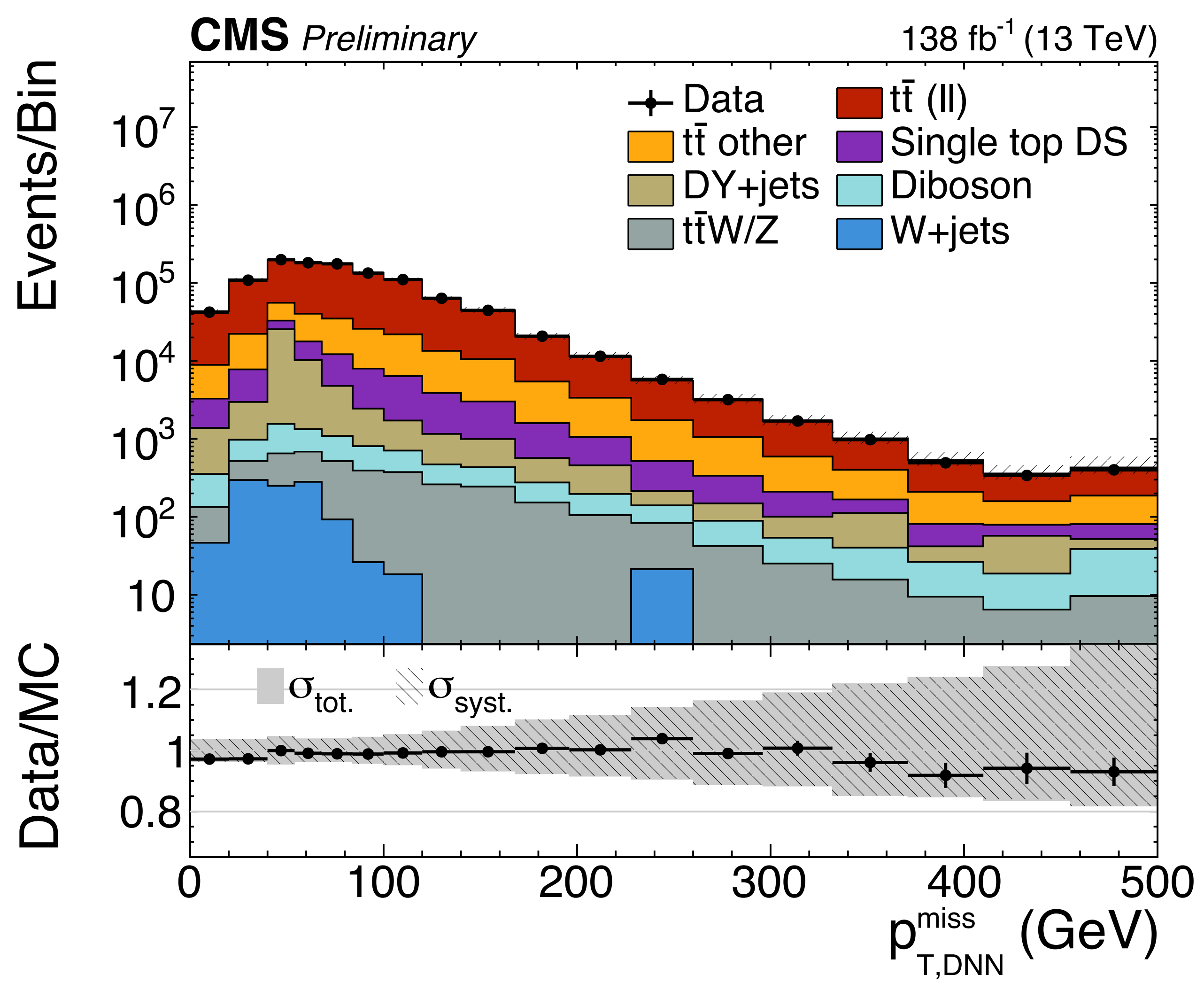

Figure_005-a

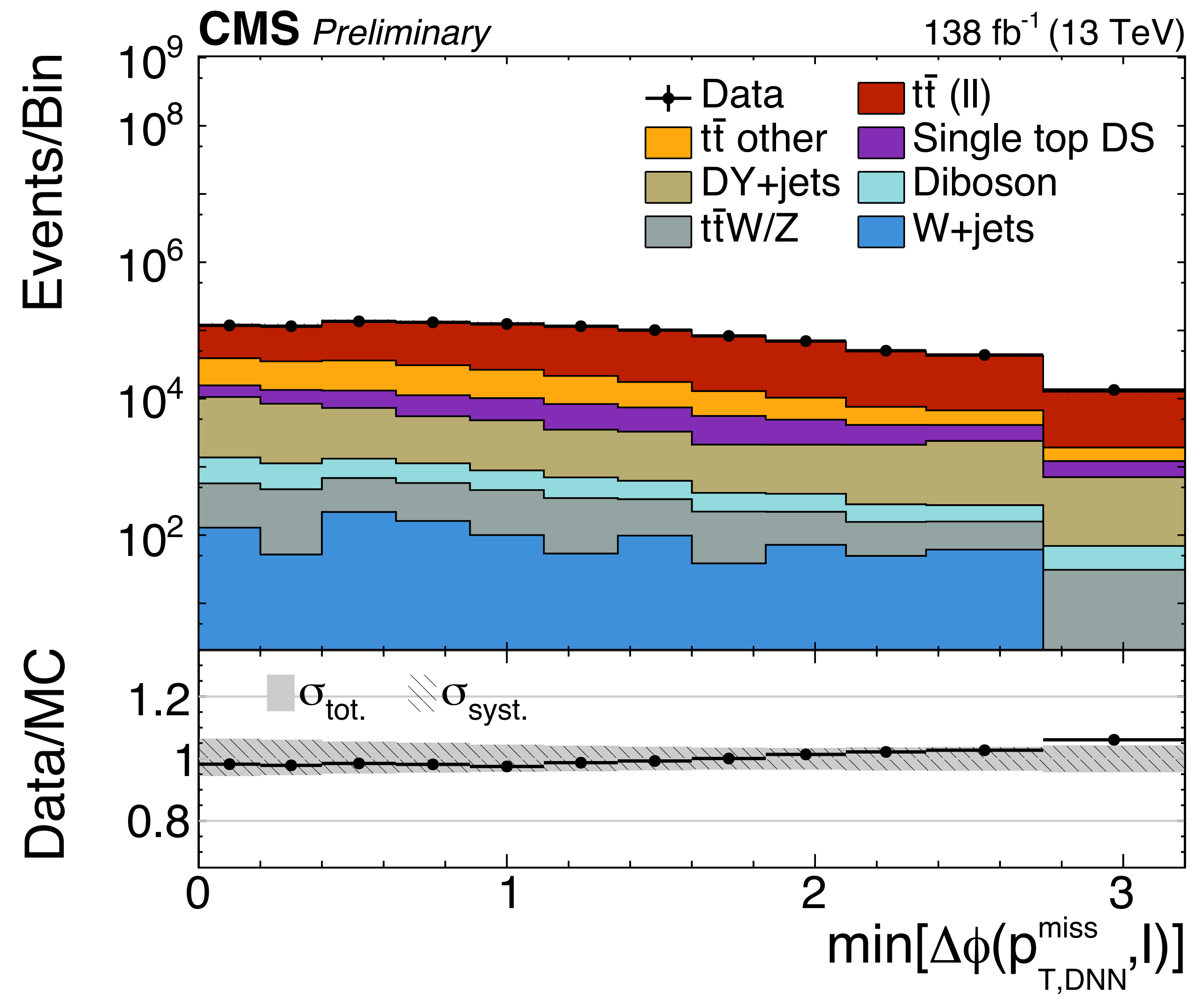

Figure_005-b

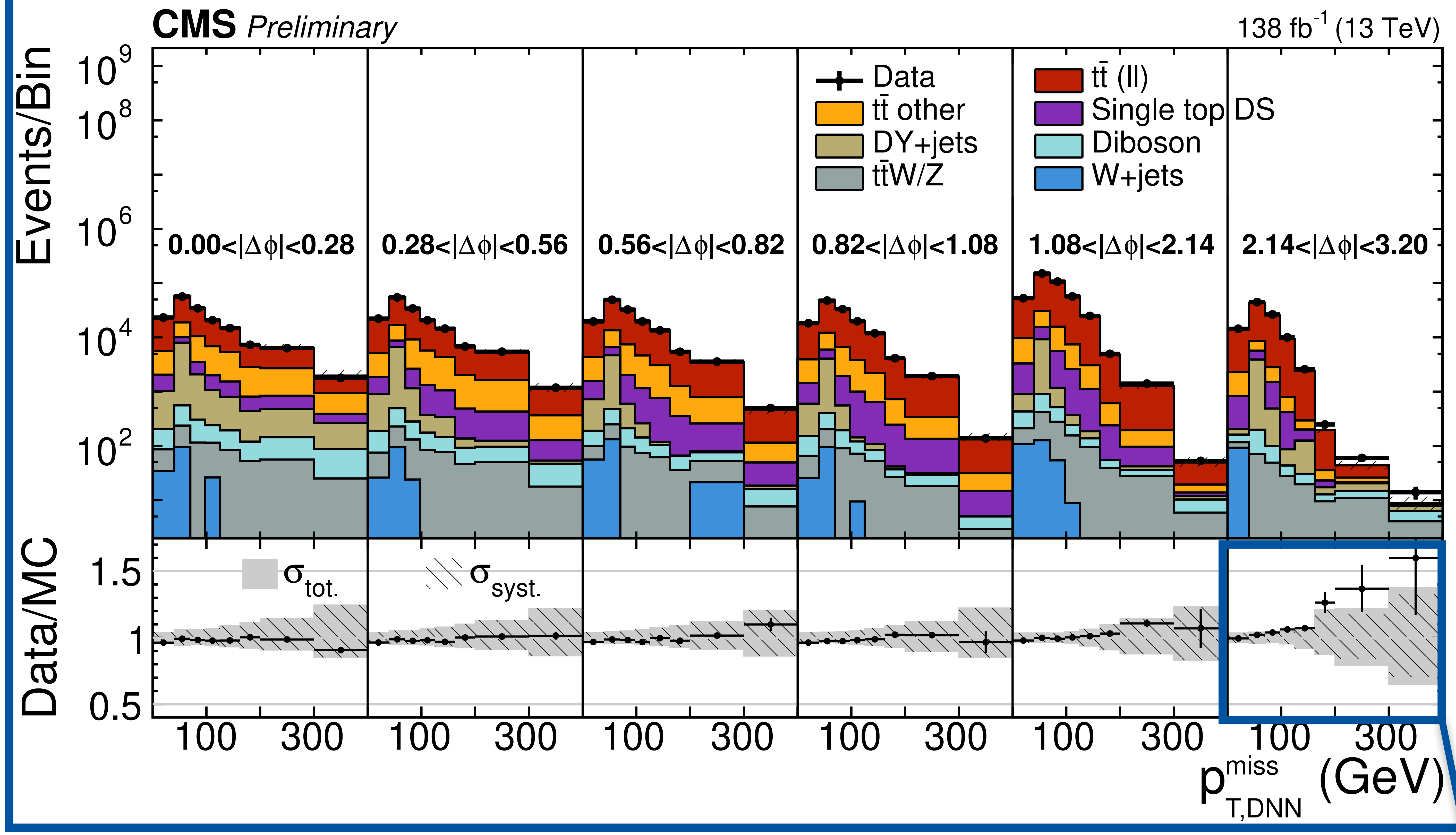

Figure_005-c

- slight over fluctuation at large $\min[\Delta\phi(\vec{p}^{\,\text{miss}}_{\text{T,DNN}}, \vec{p}^{\,\ell}_{\text{T}})]$ & $\vec{p}^{\,\text{miss}}_{\text{T,DNN}}$ found in data
- compatible with simulation considering the large statistical uncertainties in this phase space

BSM Closure test

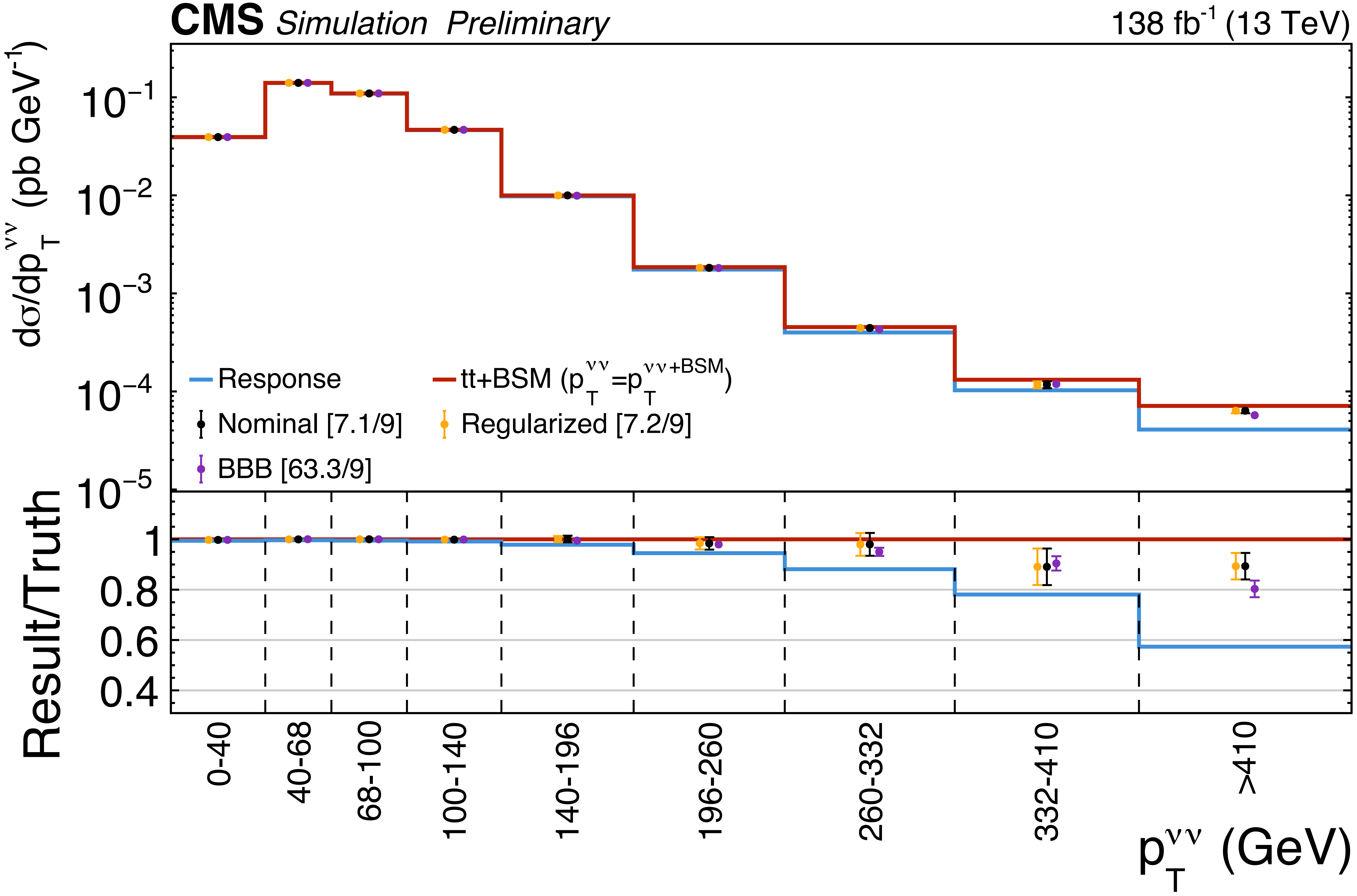

Figure_006

- **potential BSM contributions** based on stop pair production scenario:
  - ⋆ stop mass: 525 GeV
  - ⋆ neutralino mass: 350 GeV
- **pseudodata based on:**
  - ⋆ nominal $t\bar{t}$ signal prediction
    +
  - ⋆ prediction for stop pair production scenario scaled by factor of ten
- **nominal, regularized & bin-by-bin unfolding**
  - ⋆ based on all data-taking periods combined
- nominal distribution used for response matrix (blue)

PAS-TOP-24-001

BSM Closure test

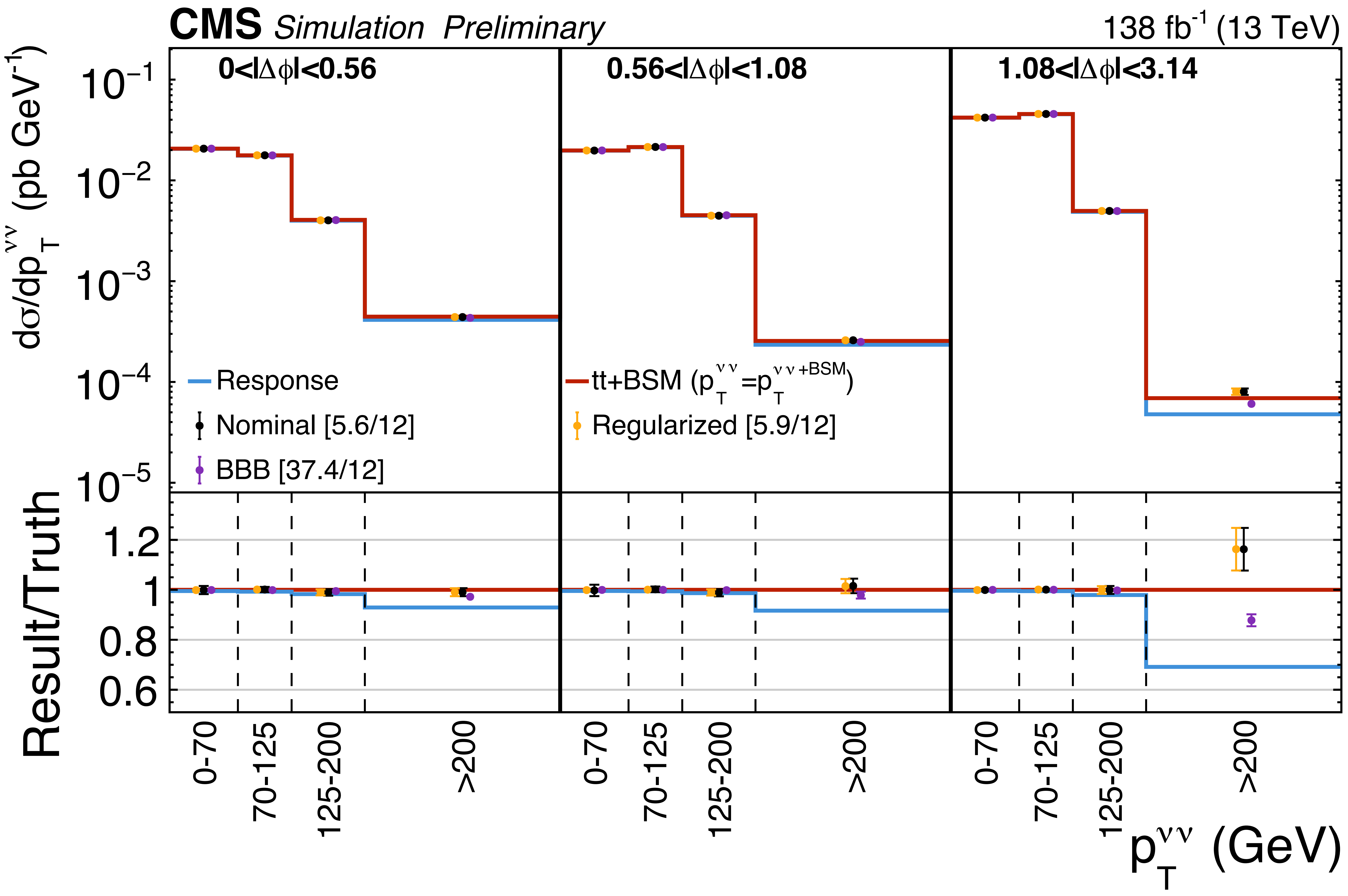

Figure_006

- expected distributions with both neutralinos included in particle level definition correctly reproduced

★ reasonable sensitivity to distortion in measured spectrum from potential BSM contributions

PAS-TOP-24-001

Differential cross-sections: $\vec{p}_{\mathbf{T}}^{\nu\nu}$

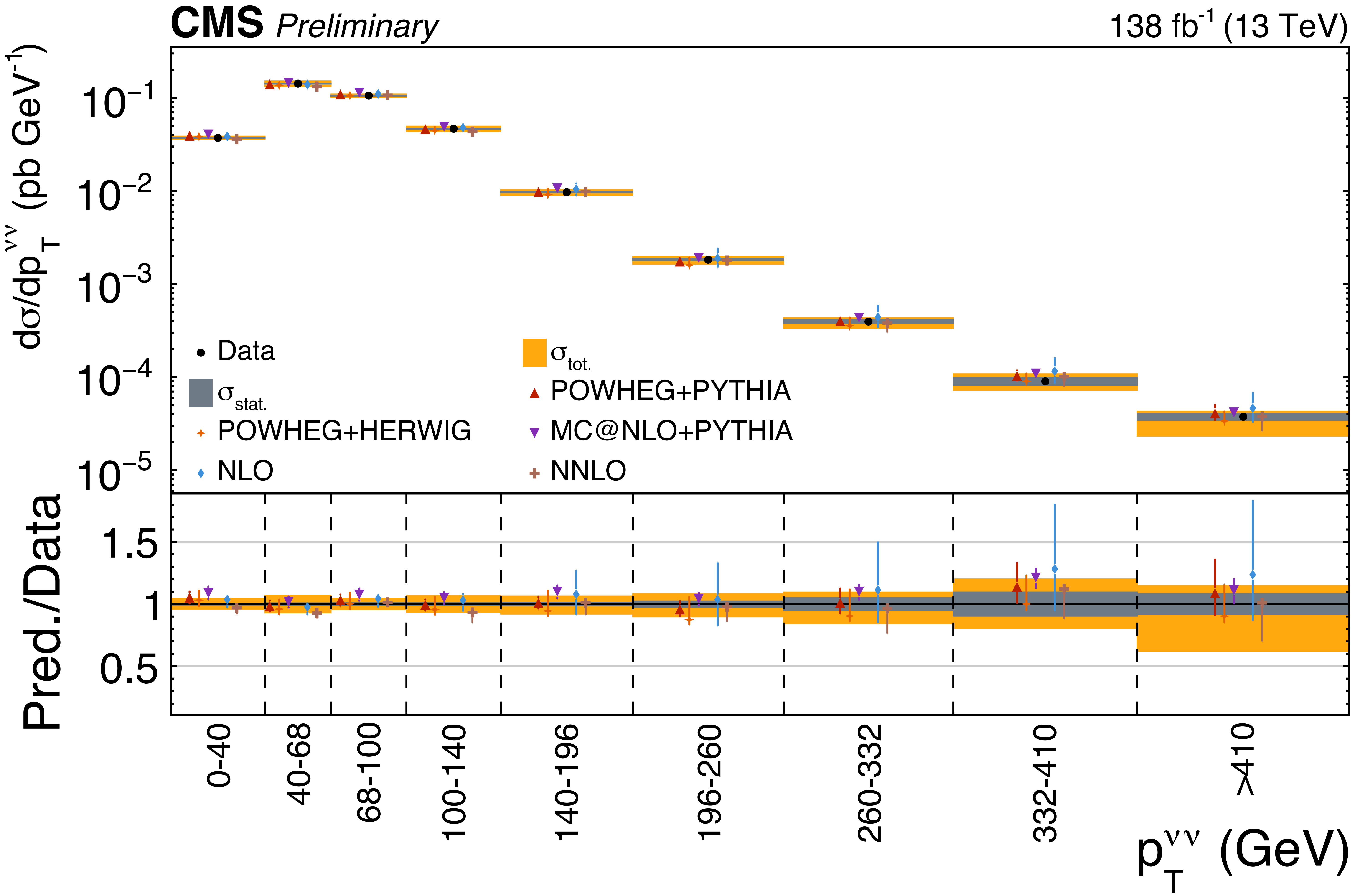

Figure_007-a

- Ratio between theoretical predictions & measurement in bottom pannel
- Total (statistical) uncertainty on measurement in orange (dark grey)
- χ^2 tests for all measurements, both with & without inclusion of uncertainties on predictions for quantitative assessment of agreement (see backup for detailed summary table)

- Fixed-order theory calculations at NLO and NNLO: 10.1007/JHEP05(2021)212

PAS-TOP-24-001

Differential cross-sections: $\min[\Delta\phi(\vec{p}_T^{\nu\nu}, \vec{p}_T^{\ell})]$

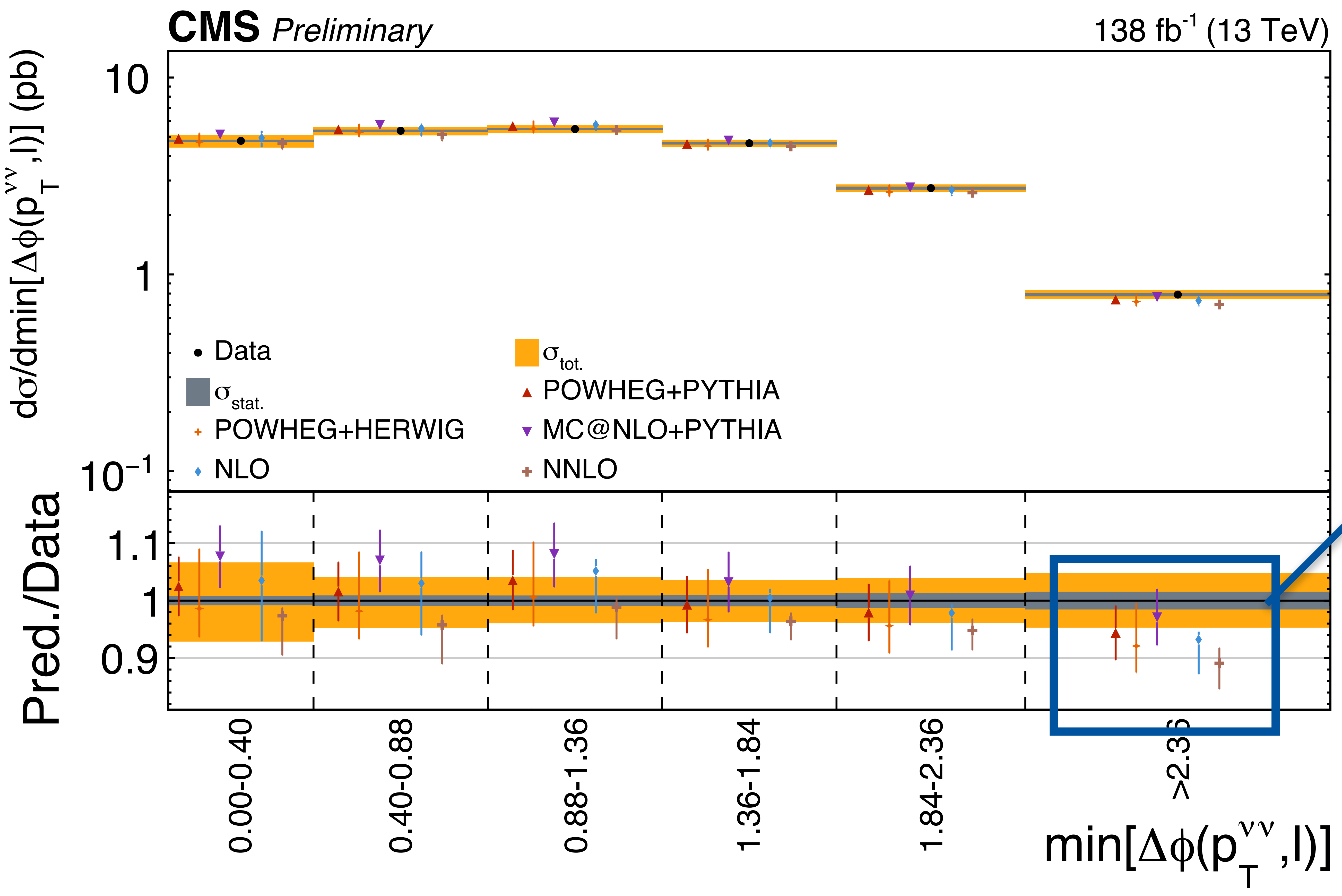

Figure_007-b

- Small shape differences between measured cross-section & five predictions
- Differences match observations from previous measurements of azimuthal angle between two leptons, strongly correlated with $\min[\Delta\phi(\vec{p}_T^{\nu\nu}, \vec{p}_T^{\ell})]$

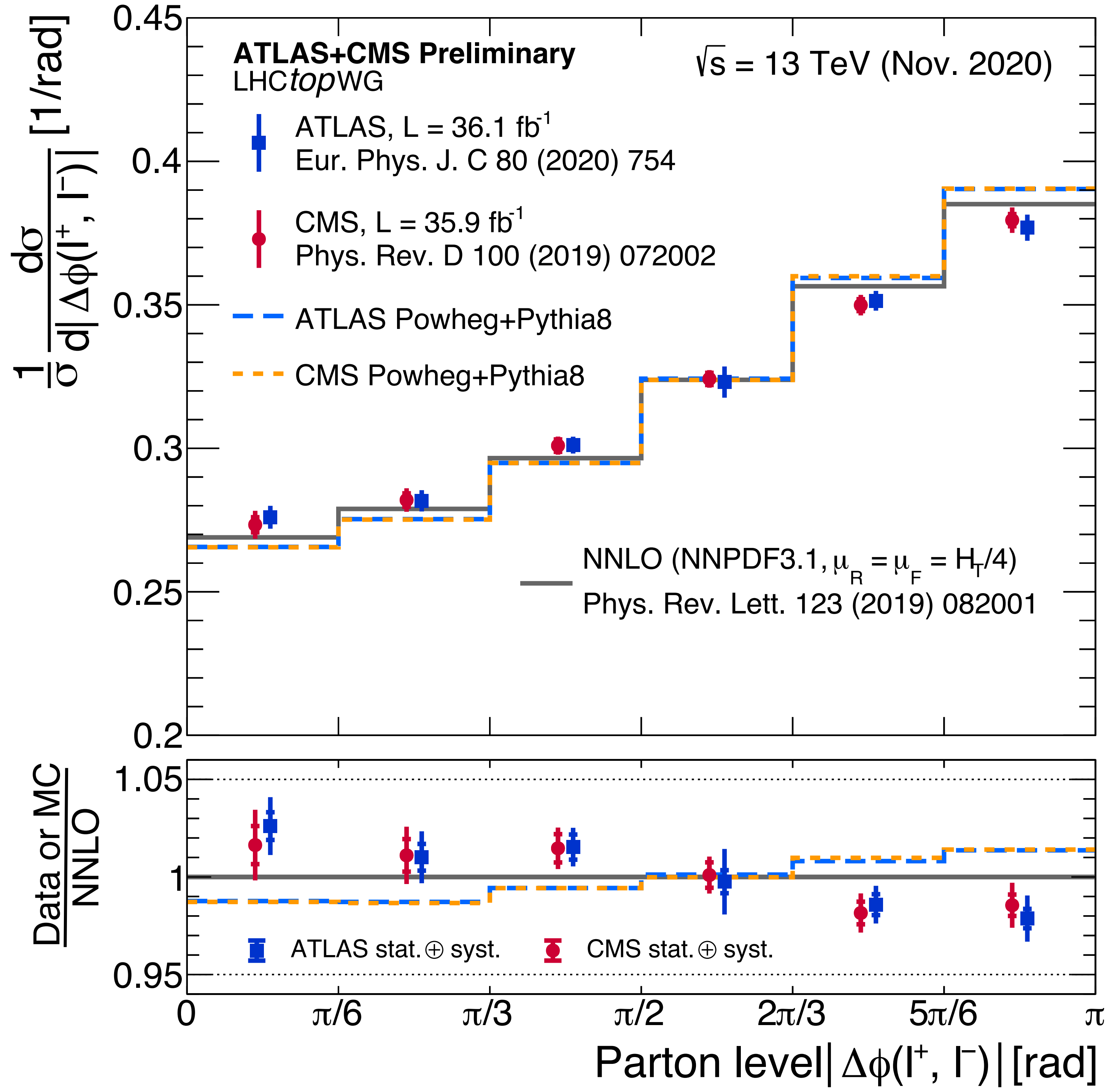

deltaPhi-NNLO

- Fixed-order theory calculations at NLO and NNLO: 10.1007/JHEP05(2021)212

Differential cross-sections: 2D distribution

PAS-TOP-24-001

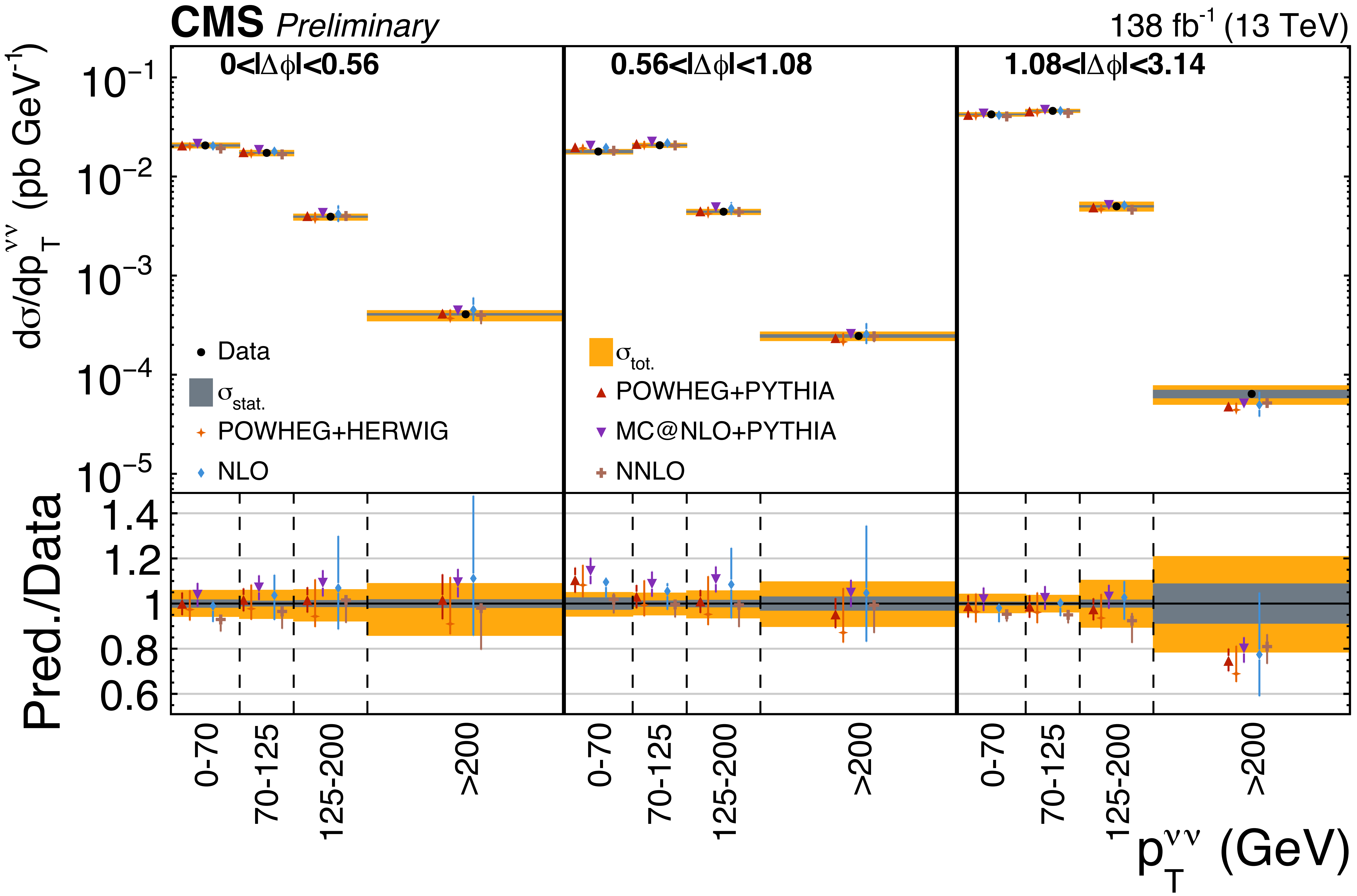

Figure_007-c

- Slightly larger χ^2 values wrt to one-dimensional distributions
- Good agreement for NNLO & POWHEG across most parts of phase space with NNLO calculation showing best agreement
- Only MC@NLO+PYTHIA prediction leads to χ^2/ndf values well above unity

- Fixed-order theory calculations at NLO and NNLO: 10.1007/JHEP05(2021)212

Summary

First differential cross section measurements based on dineutrino kinematics in top pair production

- **Absolute & normalized differential cross-section results based on unregularized least square unfolding method**

Main analysis result

  - Differential cross sections compared to predictions based on MC simulation & two fixed-order theory calculations (corresponding to NLO & NNLO in QCD)
  - Dedicated DNN regression significantly improving resolution of magnitude & azimuthal angle of missing transverse momentum

- Remarkable agreement between different theory predictions & measured differential cross sections
  - For both one-dimensional measurements, best overall description provided by POWHEG
  - For two-dimensional measurement best agreement provided by NNLO fixed-order calculation

Thank you!

Contact

Lehrstuhl für Experimentalphysik
I B und I. Physikalisches Institut
RWTH Aachen
https://www.rwth-aachen.de/

Sandra Consuegra Rodríguez (RWTH Aachen)
0000–0002–1383–1837
CMS, Higgs & Top Physics, Detector Calibration
sandra.consuegra.rodriguez@rwth-aachen.de
+49–241–80-28721
Personal website:
https://sconsueg.web.cern.ch/sconsueg/

Backup

> Additional material

Distributions after event selection

- Clean selection with overall ~78% signal contribution
- Largest background contributions from $t\bar{t}$ other, single top, and DY+jets

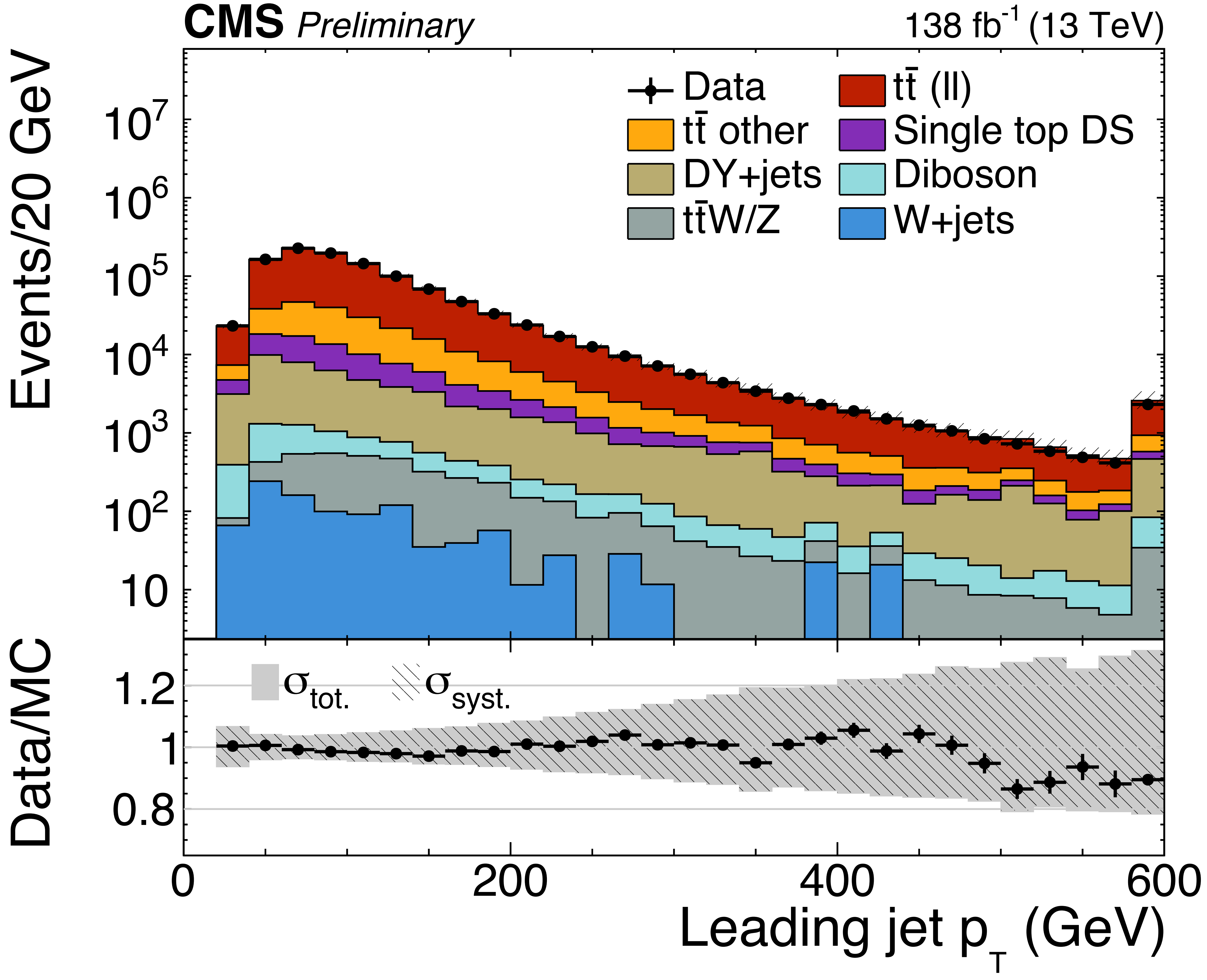

Figure 002-b

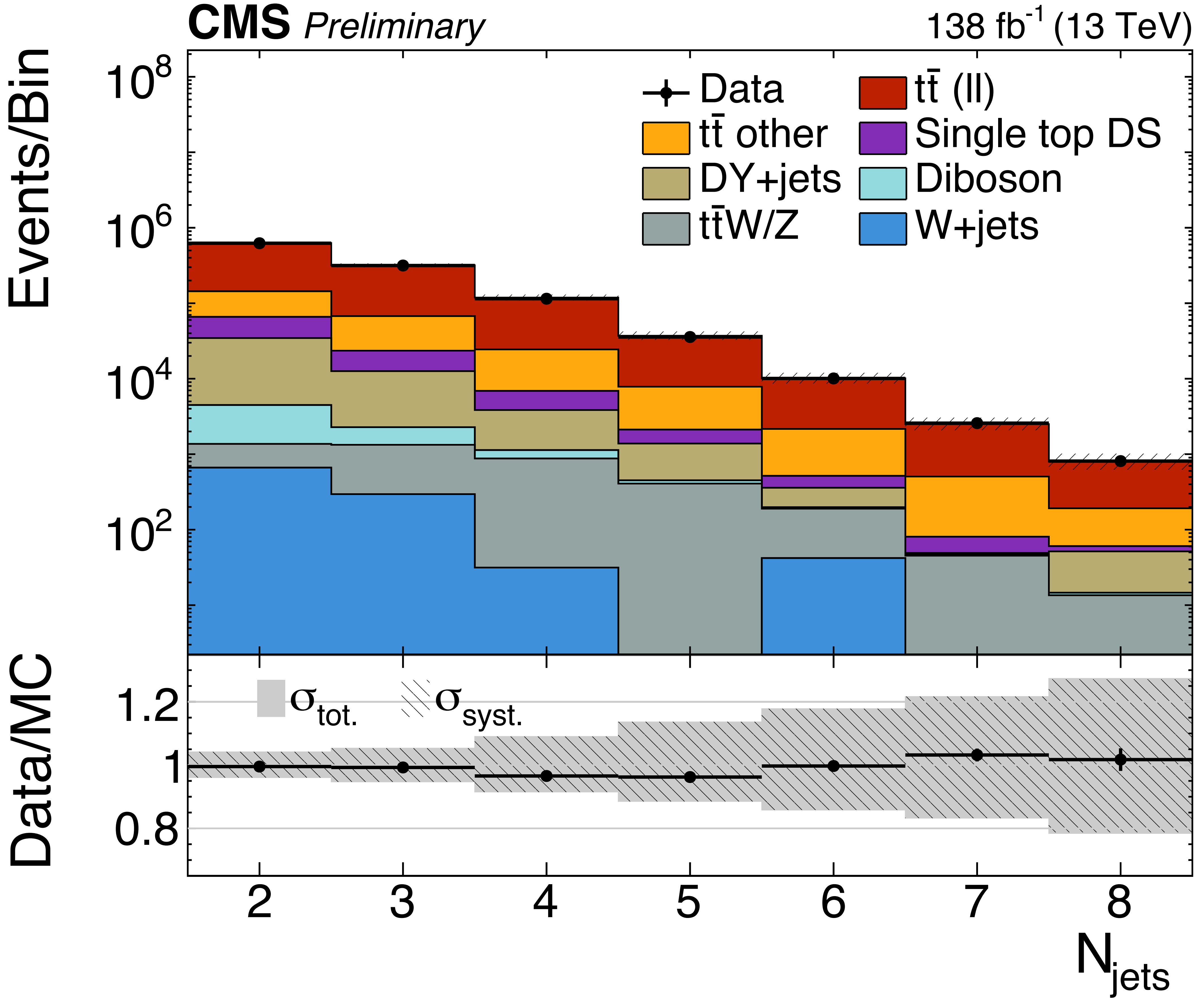

Figure 002-c

- Excellent Data/MC agreement, for individual channels & combination, and across different distributions

[PAS-TOP-24-001]

χ^2 tests for differential cross section measurements

Measurement	ndf	POWHEG +PYTHIA	POWHEG +HERWIG	MC@NLO +PYTHIA	NLO	NNLO
$p_{\mathrm{T}}^{\nu\nu}$	9	6.8 (1.6)	8.0 (1.0)	9.0 (3.9)	7.1 (1.4)	12.5 (2.5)
$\min[\Delta\phi(p_{\mathrm{T}}^{\nu\nu}, \ell)]$	6	7.3 (1.5)	7.4 (1.4)	11.5 (2.7)	12.3 (2.5)	11.9 (4.0)
2D	12	18.8 (4.9)	22.4 (3.7)	31.6 (8.6)	24.0 (3.5)	15.8 (4.2)
norm. $p_{\mathrm{T}}^{\nu\nu}$	8	6.4 (3.8)	8.3 (3.2)	6.4 (5.8)	6.7 (1.9)	13.3 (5.5)
norm. $\min[\Delta\phi(p_{\mathrm{T}}^{\nu\nu}, \ell)]$	5	7.2 (7.0)	7.2 (6.7)	9.2 (8.4)	11.7 (5.4)	11.7 (5.8)
norm. 2D	11	18.1 (16.0)	21.4 (14.5)	28.2 (22.8)	23.1 (7.0)	14.8 (8.5)